Measured and Calculated Stress in a Ribbon Parachute Canopy

William L. Garrard,* Michael L. Konicke,† K. S. Wu,‡ and K. K. Muramoto§
University of Minnesota, Minneapolis, Minnesota

An experimental study of the steady-state stresses in a model ribbon parachute canopy is presented. Using Omega sensors, the distribution of circumferential stress in the horizontal ribbons of the parachute was measured, as well as canopy pressure distribution, shape, and drag. The stress distribution and shape were calculated for the parachute canopy using the parachute structural analysis code CANO. It was found that the stresses calculated using CANO were larger than the measured stresses and that the calculated canopy shape was substantially different from the measured shape. A modified version of CANO was developed that gave a better representation of the canopy shape and stress than the original version of CANO.

Introduction

An important area in parachute technology is the development of accurate methods for determining structural loads in parachute canopies. If these loads are underestimated, system failures may result; if they are overestimated, parachutes of excessive weight and volume may be designed. In 1919, the first theoretical investigations of parachute canopy shapes and stresses were carried out at the Royal Aircraft Establishment by Taylor et al.[1] They determined the shape of a solid cloth parachute having the least weight. An axisymmetric parachute with an infinite number of suspension lines, zero circumferential stress, and uniform differential pressure distribution was assumed. Stevens and Johns[2] investigated the problem of a solid parachute canopy with a finite number of suspension lines. They arrived at the Taylor equation for the shape of the surface formed by the radials; however, they found the stresses to be only circumferential. Their analysis also showed that finite stresses exist at the canopy apex; however, infinite stresses were predicted at this point using Taylor's model. Duncan et al.[3] pointed out that the singularity in Taylor's model disappeared if the elasticity of the fabric was taken into account.

Jaeger et al.[4] investigated conical ribbon parachutes. They developed a method for determining the maximum horizontal ribbon and radial tape stresses in an axisymmetric canopy under a uniform pressure distribution. Since the Taylor shape was a poor approximation of the shape of an inflated conical canopy, Jaeger et al. assumed the canopy to be a combination of a cone with a meridional stress and an ellipsoid with zero circumferential stress. Topping et al.[5] modified Taylor's equation to take into account the gore fullness and obtained analytical solutions for the fully inflated shapes of a variety of solid parachute canopies under uniform pressure distributions. These canopies had a rounded apex rather than the flat top of the Taylor shape. Radial tensions and cloth stresses corresponding to these theoretically determined shapes were also calculated. This work was followed by Lester's analysis[6] of a generalized form of the Taylor shape equation.

Heinrich and Jamison[7] developed a method for calculating the unsteady stress distribution in an inflating solid parachute canopy. They assumed that, during the inflation process, the radial cord profile could be represented by the canopy shape as proposed by O'Hara[8] and that the instantaneous pressure differential obtained from steady-state wind-tunnel experiments could be used. The stress magnitudes predicted using this method were not high enough to account for the observed failures. Asfour[9] attributed these low stresses to the static equilibrium conditions assumed for the intermediate stages of inflation. He proposed a mathematical model of an inflating solid parachute canopy in which the circumferential stress was a result of a dynamic force in a plane normal to the flight path. By equating the energy absorbed by the cloth to the kinetic energy of the air in the radial direction, he was able to compute a circumferential stress that could account for the observed failures.

In all of the canopy stress analyses discussed above, the canopy shape was assumed to be known. Analytical techniques for simultaneously determining the canopy shape and stress distribution have been developed only since the late 1960s. Ross[10] presented an approximate theory for a solid parachute in steady descent in 1970. In this analysis, the canopy shape and stress are governed by a nonlinear third-order system of differential equations with boundary conditions at the vent and the skirt. Roberts[11] postulated a more rigorous interconnection between the stresses and the pressure distribution acting on the canopy and derived a simultaneous set of wave equations governing the inflation of a parachute canopy. Roberts then simplified and solved these equations for an arbitrary pressure distribution. Numerical results are given in Ref. 12.

In the late 1960s and early 1970s as part of the Apollo program, Mullins and Reynolds and their co-workers developed a finite-element computer code called CANO to calculate the canopy shape, stresses in the horizontal ribbons, forces in the radial members, and suspension lines for slotted parachutes.[13] CANO has been widely used in the design of high-performance ribbon parachutes[14] and, although not originally developed to simulate solid parachutes, has recently been used for this purpose.[15] The code did not originally include the effects of vertical elements, but was later modified to simulate the effects of verticals on the parachute shape by including fictitious distributed forces on the edges of the

Presented as Paper 84-0816 at the AIAA 8th Aerodynamic Decelerator and Balloon Technology Conference, Hyannis, MA, April 2-4, 1984; received July 1, 1985; revision received Sept. 25, 1986.

*Professor, Department of Aerospace Engineering and Mechanics. Associate Fellow AIAA.

†Research Assistant, Department of Aerospace Engineering and Mechanics (currently with Boeing Co., Seattle, WA). Member AIAA.

‡Research Specialist, Department of Aerospace Engineering and Mechanics (currently with Nanjing Parachute Co., Nanjing, China).

§Research Assistant, Department of Aerospace Engineering and Mechanics (currently with Acurex Aerotherm Co., Mountain View, CA).

horizontal ribbons.[16] In practice, this modification often caused convergence problems and has not been used extensively.

The required inputs for CANO are 1) the parachute geometry, including the number of gores, gore dimensions, ribbon widths and heights, slot widths, and suspension and vent line lengths; 2) material type and nominal breaking strength for each element; 3) nondimensional load vs strain curves for each material; 4) differential pressure coefficient distribution as a function of nondimensional distance from the vent; 5) initial guess for the canopy radius at the skirt; and 6) the axial load. Outputs include inflated canopy shape and loads in suspension lines, radials, vent lines, and horizontal ribbons. Basic assumptions are that 1) all elements are in uniaxial tension and static equilibrium; 2) horizontal elements are arcs of circles; 3) radials are perpendicular to horizontal elements at the attachment points; 4) all gores are identical; 5) effects of verticals are ignored; 6) spanwise pressure distribution across a given element is uniform and is balanced by the hoop stress in the element; and 7) force due to pressure on the radials is negligible. The pressure distribution on an element is determined by linear interpolation from a limited number of differential pressure coefficients (a maximum of nine) input to CANO. The computations are performed for a single gore.

The axial component of the suspension line loads balance the axial force input. Suspension line loads are determined by an iterative solution of the equilibrium and force/deformation equations for the suspension lines. Once the suspension line loads have been determined, computations on the canopy proceed from the skirt to the vent. The pressure on a horizontal element is balanced by the hoop stress on the ends of this element. This hoop stress is, in turn, in equilibrium with the loads in the radial elements connected to the ends of the horizontal element. The suspension lines comprise the elements attached to the lower side of the horizontal element at the skirt. The loads in the suspension lines are known because they were calculated previously to balance the axial load. The loads and geometry of the skirt horizontal element and the radials attached to the upper side of this element are then calculated using the equilibrium and compatibility between the stretched and geometrically determined length of the horizontal element. These form a coupled set of nonlinear algebraic equations that must be solved numerically. The skirt radius is iteratively adjusted until equilibrium and geometric compatibility are achieved. The calculations then proceed to the next horizontal element. The forces in the radials attached to the lower side of this horizontal are known from the calculations performed on the previous element and the geometry and forces in the horizontal, and the radial elements attached to its upper side are determined in the same manner as for the skirt horizontal. The calculations proceed sequentially to the vent.

Once the vent is reached, the force due to the pressure on the vent hole is calculated. If the calculated axial force component due to the radials converging at the vent is not 25-75% of the pressure force on the vent hole, then the magnitude of the differential pressure coefficient distribution is adjusted and the calculations for the entire canopy are repeated. If the axial force lies between the specified limits, the vent line length is calculated from both the canopy geometry and the force/deformation relationship for this element. If these two lengths are not sufficiently close to one another, the magnitude of the skirt radius is modified and the calculations for the entire canopy are repeated. If they are acceptably close, CANO is considered to have converged. This may require a large number of iterations. CANO is described in detail in Ref. 23.

Since there has not been an experimental verification of CANO, one of the primary objectives of the study described in this paper was to measure the axial force, pressure, and stress distributions and the shape of a model ribbon parachute canopy in the wind-tunnel and compare the measured shape and stress distribution with the shape and stress calculated using CANO. The model ribbon parachute used in the wind-tunnel tests was 18 in. in diameter. This parachute was instrumented with Omega sensors[17-22] for stress measurements and taps for pressure measurements. The ambiguities involved in calibrating the Omega sensors were resolved by using the sensors to measure total force rather than stress in the ribbons. Force was then converted to stress by dividing by the nominal width of the ribbons. The canopy shape was measured photographically. Measurements of steady-state stress and pressure distributions, axial force, and shape were performed at several dynamic pressures. Steady-state measurements avoided the many difficulties associated with making measurements on inflating parachute canopies. Since CANO performs calculations based on the pressure distribution and axial force data supplied, steady-state results are just as useful as transient results in verifying the code.

The measured and calculated stress distributions were found to be of the same general shape, but the calculated stresses were somewhat greater than the measured stresses. The canopy shape predicted using CANO and the measured shape differed substantially. These differences were due to differences in the slope at the vent and the angle the horizontal ribbons made with the radials. The slope at the vent can be varied by changing a boundary condition; however, in the standard version of CANO, it is impossible to change the angle the horizontals make with the radials. Using the standard version of CANO, the vent slope was varied until the best approximation of the shape was found. The resulting calculated stresses were much closer than those calculated using the standard vent condition.

Since the standard version of CANO does not simulate the verticals and also does not accurately model the angles the horizontals make with the radials, a modified version of CANO called CANO3 was developed.[23] This version has an option for including verticals and allows a more accurate simulation of the shape near the skirt. The verticals are simulated as concentrated loads—not as fictitious distributed loads as in a previous modification of CANO.[16] CANO3 provided canopy shapes and stress distributions that were very close to the measurements.

In addition, several modifications were made in the original version of CANO that improved the convergence properties. CANO and CANO3 were revised to run on microcomputers and to be more user friendly than the original version.[23] Since many parachute designers do not have access to large mainframe computers of the type for which CANO was originally developed, it is felt that these microcomputer versions of CANO may be very useful in the parachute industry.

Experimental Procedures

The model parachute used in the experimental study was a flat, 18-in. nominal diameter, cut-gore, ribbon parachute of 25% geometric porosity. This parachute was constructed of eight gores and had eight suspension lines which were 31 in. long ($L/D=1.77$). Each gore had nine horizontal ribbons and two verticals. The horizontal ribbons were 0.675 in. in width and were constructed of nylon tape of 90-lb nominal breaking strength. The slots between ribbons were 0.25 in. in width. The verticals were constructed of 58-lb nominal breaking strength nylon tape, the radials of two plies of 90-lb nominal breaking strength nylon tape, and the suspensions lines of 400-lb nominal breaking strength round, braided nylon cord. Vent and skirt ribbons were reinforced with an additional ply of 90-lb nominal breaking strength nylon tape and the pocket bands were simulated. Except for the scaling of the material properties and gore component spac-

ing, the construction of the parachute was similar to that of full-scale, cut-gore, ribbon parachutes. The parachute flew at an angle of attack of 0 deg and exhibited very little motion about this condition when in the wind tunnel.

All testing was performed in the open section of the University of Minnesota low-speed wind tunnel. The open section of this wind tunnel has a test section with dimensions of 5×5 ft. The flow within this section is very uniform and a maximum dynamic pressure of 9 lb/ft^2 is obtainable. The inflated diameter of the parachute was about 13 in. and the blockage ratio about 3.7%.

The parachute was mounted horizontally on a sting in the wind tunnel (Fig. 1) with the confluence point attached to a strain gage balance by means of a nylon riser. Differential pressure measurements were made at five points on the canopy using pressure taps. These taps were small brass tubes mounted perpendicular to the ribbons. Measurements were made along the gore centerline at the midchord of the ribbons. Ten taps were mounted on the parachute on alternate ribbons from the vent to the skirt. Five taps were mounted facing the interior of the canopy and five facing the exterior. Small neophrene tubes were attached to the pressure taps. These tubes were sewn to the parachute and passed along the sting to a pressure transducer. One of the pressure taps mounted on the exterior of the parachute canopy is shown in Fig. 2. The tubes from the exterior and interior pressure taps on a given ribbon were attached to a pressure transducer and the differential pressure was measured. The output of the transducer was digitized and input to a microcomputer that calculated the average and standard deviation for each set of measurements. This was performed for each set of taps. The dynamic pressure in the wind tunnel was also measured. Measurements were checked using a micromanometer. The differential pressures measured were 7.33–12.37 lb/ft^2. The differential pressure coefficients were calculated by dividing the differential pressure at each ribbon by the dynamic pressure in the wind tunnel. Measurements were performed at dynamic pressures of 5.2, 6.5, and 7.8 lb/ft^2. Although the dynamic pressures were low for a parachute of the structural strength of the wind-tunnel model, the inflated shape was normal and there were no large crimps or creases in the ribbons. The inflated parachute is shown in Figs. 3 and 4.

Henfling and Purvis[24] showed that substantial variations in pressure can occur in both the spanwise and chordwise directions on a single ribbon. However, in a previous study, pressure measurements were taken on a ribbon parachute similar to the one used in this study. Pressures were measured both along a gore centerline and along a radial.[25] The magnitudes of the two pressure distributions were different, but the general shapes of the curves were similar. These pressure distributions were used in CANO to calculate the stress and the resulting stress distributions were similar. This is because CANO adjusts the magnitude of the pressure coefficient curve during the computations to satisfy the vent boundary condition. Thus, the absolute magnitude of this curve is not important and, as long as the shapes of the pressure distributions are similar, the resulting stress distributions will also be similar, the resulting stress measurements were taken along the gore centerline, it seemed appropriate to make the pressure measurements there also. Furthermore, CANO assumes a constant spanwise pressure distribution across an element and performs a linear interpolation in the chordwise direction across a ribbon and cannot accept more realistic distributions. Based on these facts, it was felt that pressure measurements taken on the gore centerline at the ribbon midchord points were adequate for the purpose of verifying the accuracy of CANO.

Stress measurements were accomplished using Omega sensors.[17–22, 25–27] Six Omega sensors were mounted on the

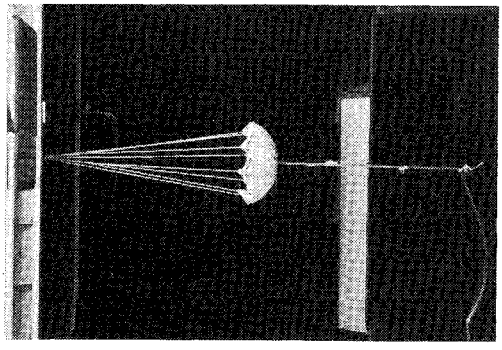

Fig. 1 Model parachute mounted in wind tunnel.

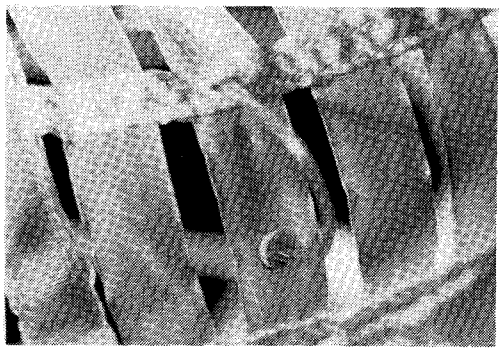

Fig. 2 Pressure tap mounted on exterior of parachute.

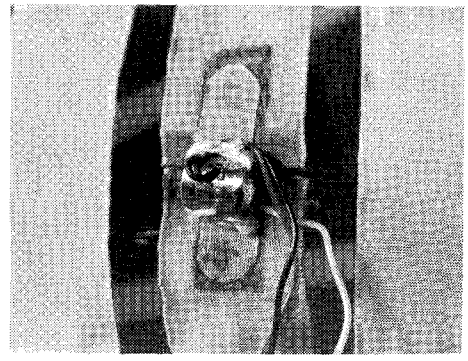

Fig. 3 Omega sensor mounted on ribbon.

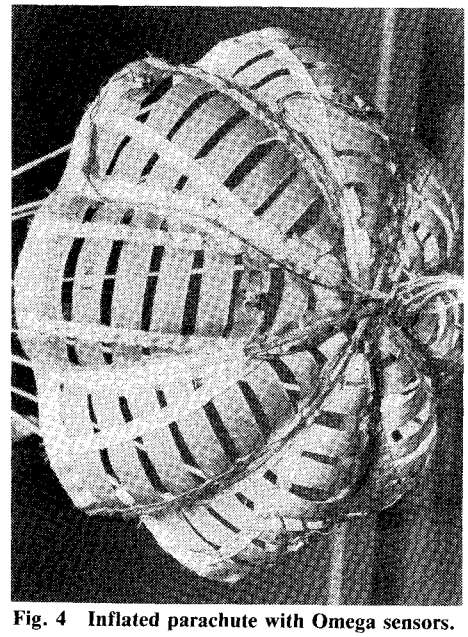

Fig. 4 Inflated parachute with Omega sensors.

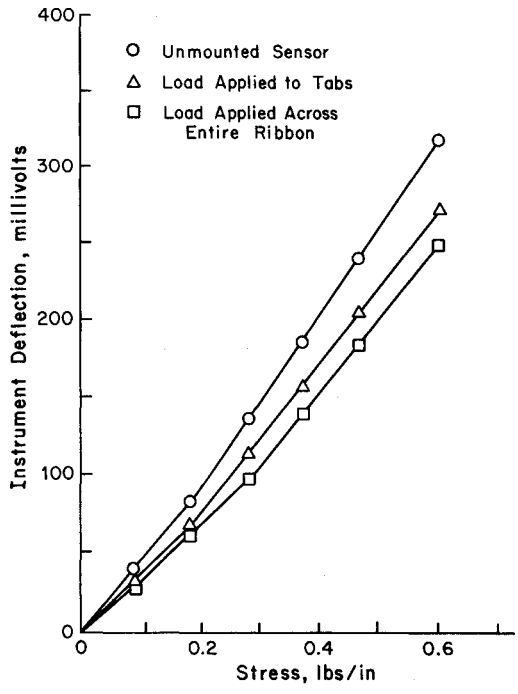

Fig. 5 Omega sensor output for various loading conditions.

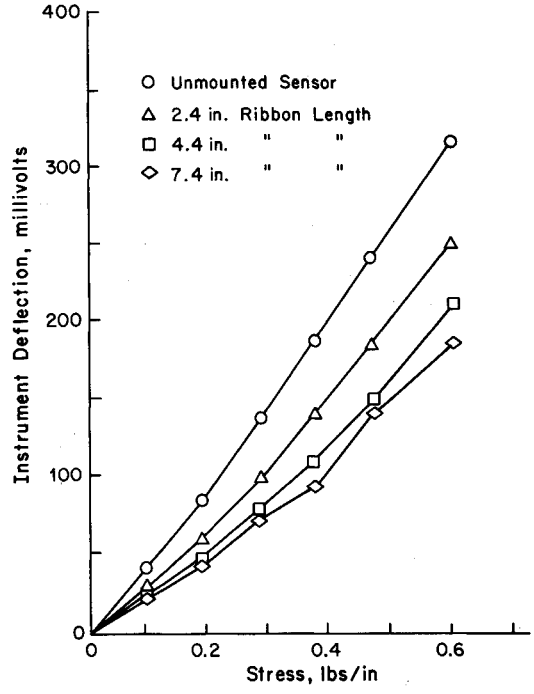

Fig. 6 Omega sensor output for various ribbon lengths (load applied across entire ribbon).

parachute. Since the parachute had nine ribbons, 67% of the ribbons were instrumented. In previous studies, Omega sensors were attached to the parachute canopy with cloth tabs and a small slit the width of the sensor was cut in the ribbon under the sensor.[17-22, 25-27] The sensors were then calibrated by attaching known weights to the tabs and measuring the strain gage outputs from the Omega sensors. The basic assumption underlying this calibration procedure was that the output of the sensor was independent of how the tensile stress was applied. This is not the case, as is shown in Figs. 5 and 6, which illustrate the results of a series of experiments in which Omega sensors were attached to cloth ribbons of different sizes and elastic properties. A slit was cut under the Omega sensors, the ribbons were subjected to uniaxial stress in various ways, and the outputs of the Omega sensors were recorded. Figure 5 shows the effects of different methods of applying stress to an Omega sensor. When the stress was applied directly to the sensor tabs before the sensor was mounted on the cloth, the calibration curve was significantly different than when the sensor was mounted to the cloth and stress was applied to the tabs. When the same stress was applied uniformly across the entire width of the ribbon, the calibration curve was significantly different than when the same stress was applied across the tabs only. All of these calibration curves are linear; however, their slopes differ considerably. Figure 6 shows the effect of different ribbon lengths on the Omega sensor output. Stress was applied uniformly across the ribbon. As the length of the ribbon was increased, the calibration curve changed significantly. For longer lengths, the curves tended to converge, although some loss of linearity resulted. This indicates that if the ribbons are sufficiently long, the Omega sensors may provide a reasonably accurate measure of the far-field stresses. Unfortunately, the model parachute used in this study is small enough that the ribbons, especially in the vent region, are so short that the traditional method of mounting and calibrating the Omega sensors yields questionable results.

The difference in elastic modulus between the cloth and the sensor appears to be the principal factor in causing the variations discussed above. If the elastic modulus of the sensor were the same as that of the cloth, the calibration results for the various configurations should be the same. It was impossible to construct Omega sensors that had an elastic modulus approaching that of the ribbons of the model parachute and also sufficient sensitivity to measure the low-stress levels encountered during the wind-tunnel tests.

The calibration problem was solved by completely cutting the ribbon on which the stress was to be measured and using the Omega sensor to reattach the two halves. All of the force was then transmitted through the Omega sensor and the calibration should have been independent of ribbon size, elastic properties, and method of loading. Experiments proved this to be the case. The resulting calibration curves were indistinguishable from those for the unmounted sensor regardless of ribbon length, width, or method of applying stress (Figs. 5 and 6). Since dynamic pressures were low, the inflated shapes of the ribbons on which the sensors were mounted were not significantly different from those on which no sensors were mounted. Figure 3 shows an Omega sensor mounted on a ribbon of the inflated parachute and Fig. 4 the entire parachute with Omega sensors. The load/strain curves for the ribbons, radials, verticals, and suspension lines measured at the low-stress levels encountered in the wind-tunnel tests were then used in the CANO calculations. Since the Omega sensor cannot be used to simultaneously measure biaxial stress at a single point, a stress transducer proposed by Testa and Boctor[28] might be useful for solid parachutes. As with the Omega sensor, this gage would be accurate in measuring only the far-field stresses and thus the parachute would have be relatively large if an accurate stress distribution were to be obtained.

The Omega sensors were calibrated as described above and the parachute was mounted in the wind-tunnel. Zero stress readings were taken on the uninflated parachute. The wind-tunnel was then run up to the desired pressure and the stresses were measured. During each test, 120 data points were taken from each Omega sensor. Total data collection time was 94 s. After data collection was complete, the wind-tunnel was shut down and the zero stress readings were taken again. The tests were conducted as rapidly as possible in order to minimize any zero shifts caused by the heating of the Omega sensors due to the strain gage excitation currents.[22] Stresses were calculated using the average of the zero readings taken before and after each test. The strain gages

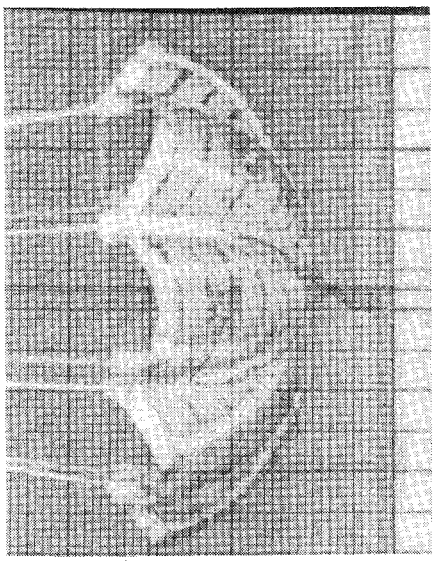

Fig. 7 Inflated parachute with grid.

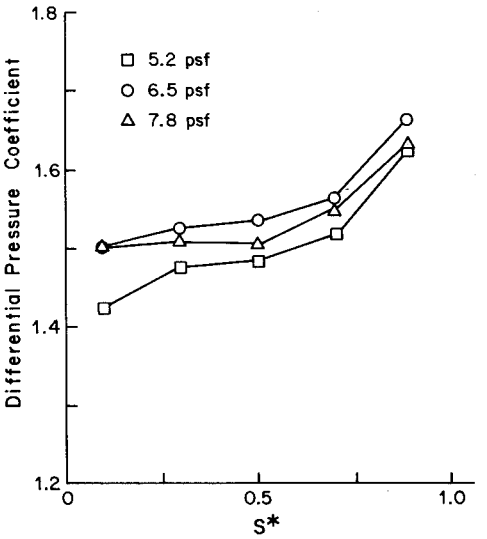

Fig. 8 Differential pressure coefficients vs S^*.

Table 1 Differential pressure coefficients

		C_p					
Ribbon		5.2 lb/ft^2		6.5 lb/ft^2		7.8 lb/ft^2	
No.	S^*	Avg.	Std. dev.	Avg.	Std. dev.	Avg.	Std. dev.
1	0.125	1.41	0.01	1.48	0.04	1.48	0.04
3	0.345	1.46	0.08	1.50	0.01	1.49	0.09
5	0.545	1.47	0.06	1.53	0.07	1.48	0.07
7	0.740	1.52	0.03	1.54	0.03	1.51	0.05
9	0.956	1.60	0.04	1.65	0.07	1.61	0.09

were allowed to return to ambient temperature before another test was performed. Numerous tests were performed at each dynamic pressure. Drag measurements were performed at the same time as the stress measurements.

The shape of the inflated parachute was determined photographically. A negative was made of the inflated parachute in the wind tunnel. The parachute was then removed and a large piece of cardboard upon which a grid with squares 0.2×0.2 in. had been inscribed was inserted in the wind-tunnel so that the cardboard was vertical and aligned with the axis of symmetry of the parachute. The negative was exposed again, resulting in a double exposure in which the image of the grid was superimposed on that of the parachute (see Fig. 7). The position of points on a vertical plane passing through the axis of symmetry of the parachute could then be determined. The shape of the gore centerline was obtained by placing the centerline of one of the gores in the plane previously occupied by the cardboard. The shape of the radial was obtained by rotating the parachute until one of the radials was in this plane. Only portions of the radials could be seen through the slots in the parachute; it was not possible to measure the shape of the radial near the vent.

Experimental Results and Comparison with Calculations

The experimental pressure distributions are shown in Fig. 8 and Table 1 as a function of nondimensional position S^* measured from the vent. These distributions were used in calculating the stress using the various modifications of CANO.

The results of the stress and drag measurements are shown in Table 2. The standard deviations in stress are the smallest

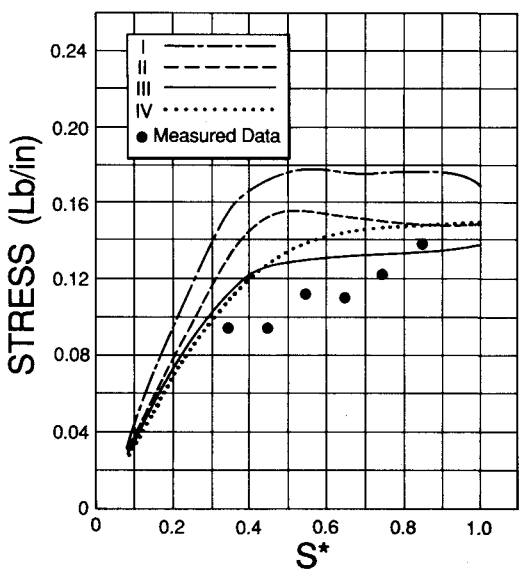

Fig. 9 Calculated and measured stress vs S^* for 5.2 lb/ft^2 dynamic pressure: I) CANO conventional vent slope, II) CANO3 conventional vent slope, III) CANO3 modified vent slope, IV) CANO modified vent slope.

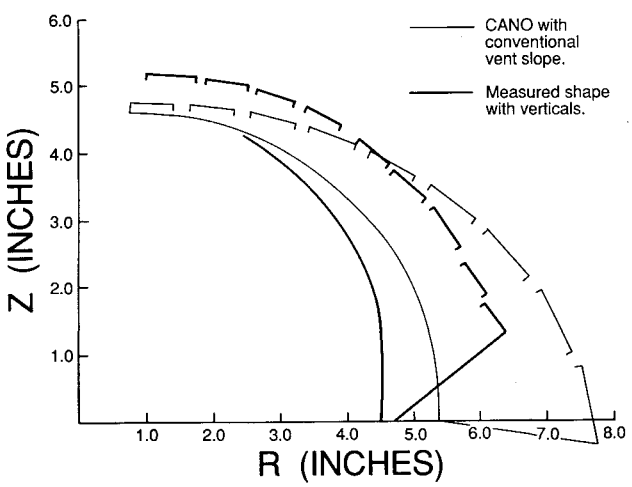

Fig. 10 Measured and calculated shapes (CANO conventional vent slope, 5.2 lb/ft^2 dynamic pressure).

Table 2 Stress and drag measurements

Ribbon No.	S^*	Stress, lb/in. 5.2 lb/ft² Avg.	5.2 lb/ft² Std. dev.	6.5 lb/ft² Avg.	6.5 lb/ft² Std. dev.	7.8 lb/ft² Avg.	7.8 lb/ft² Std. dev.
3	0.348	0.0923	0.0029	0.1315	0.0044	0.1537	0.0049
4	0.449	0.0915	0.0053	0.1185	0.0044	0.1403	0.0044
5	0.551	0.1140	0.0044	0.1309	0.0037	0.1685	0.0056
6	0.653	0.1100	0.0019	0.1288	0.0029	0.1688	0.0027
7	0.754	0.1220	0.0027	0.1534	0.0029	0.1819	0.0063
8	0.856	0.1385	0.0048	0.1743	0.0043	0.2146	0.0061
Drag, lb		5.134	0.056	6.663	0.075	8.072	0.093
Drag coefficient		0.559		0.577		0.586	

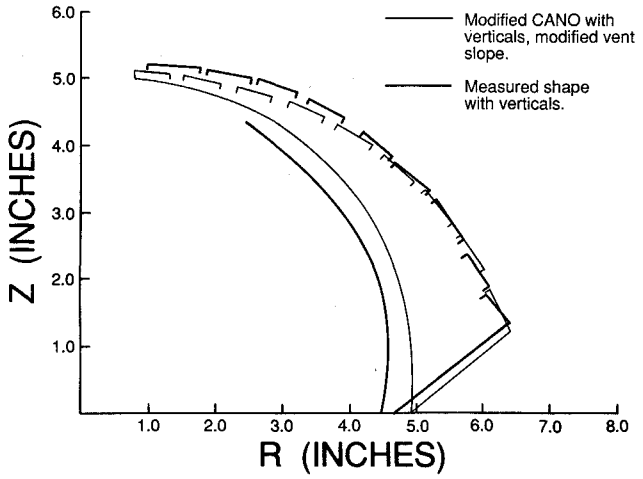

Fig. 11 Measured and calculated shapes (CANO modified vent slope, 5.2 lb/ft² dynamic pressure).

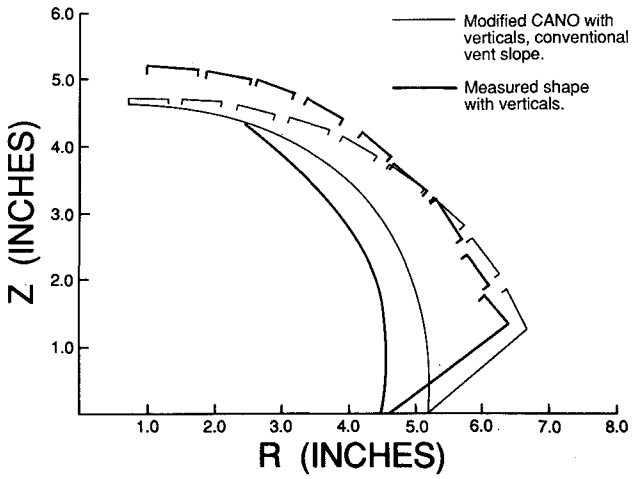

Fig. 12 Measured and calculated shapes (CANO3 conventional vent slope, 5.2 lb/ft² dynamic pressure).

yet achieved at the University of Minnesota. Measured and calculated stress is plotted vs S^* in Fig. 9 for a dynamic pressure of 5.2 lb/ft². It can be seen that CANO predicts stresses which are greater than the measured stresses. Figure 10 shows that the shape calculated using CANO is considerably different than the measured shape. The shapes differ substantially in both the vent and skirt regions. In the vent region, CANO predicts a much flatter shape than measured. Since a flat shape indicates high stress, it would be expected that CANO would predict higher stresses than were measured. This is indeed the case. In the skirt region, the two shapes are different because one of the basic assumptions of CANO is that the horizontal ribbons are perpendicular to the meridional elements. It has long been realized that this is a poor assumption, particularly in the skirt region. There was a previous attempt to modify CANO to correct this problem by simulating verticals as distributed forces along the top of the horizontal elements[16]; however, this resulted in a code with serious convergence problems.

Several things can be done to improve the ability of CANO to predict the inflated shape of the parachute. First, the boundary condition in CANO that controls the slope at the vent can be changed. In the original formulation of CANO, there is an arbitrary condition at the vent that allows iterations to stop when the calculated axial force component due to the radials converging at the vent is 0.25–0.75 times the differential pressure at the vent times the area of the vent. If these bounds are increased or decreased, the shape of the parachute is changed substantially. As the bounds are increased, the force components in the axial direction increase and, therefore, the slope of the radials at the vent must increase. Since more force is carried by the radials, the stress in the horizontal ribbons near the vent should decrease. Figure 10 shows that the measured slope of the radials near the vent is considerably greater than predicted by CANO. The bounds on the radial forces at the vent were increased until the calculated shape near the vent was close to the measured shape as shown in Fig. 11. The resulting calculated stress is shown in Fig. 9. It is much closer to the measured stress than the stress calculated using the original vent slope boundary conditions. The calculated and measured stress are farthest apart in the skirt region where the calculated and measured shapes do not agree very well. A modified version of CANO, CANO3, was developed to try and solve this problem.[23] CANO assumes the angles the horizontal elements make with the perpendiculars to the radials at the points of attachment to be zero. From Fig. 7, it can be seen that this is a poor assumption. CANO3 allows nonzero values of these angles. For stations below the point at which the verticals are attached to the radials, CANO3 adjusts these angles at each iteration until geometric compatibility with the stretched length of the verticals is achieved. For stations above the point at which the verticals are attached to the radials, each horizontal ribbon is assumed to make a constant angle with the perpendicular to the radial at the point of attachment. Empirically, a value of π/M (where M is the number of gores) appears to give good results. A listing and detailed description of CANO3 is given in Ref. 23.

The calculated shape resulting from CANO3 is shown in Fig. 12. It can be seen that the measured and calculated shapes are very similar near the skirt, but not near the vent. Since the vent boundary conditions were not changed from the 0.25 and 0.75 values used in the original CANO calculations, this is to be expected. The resulting stress distribution as shown in Fig. 9 is closer to the measured stress than is

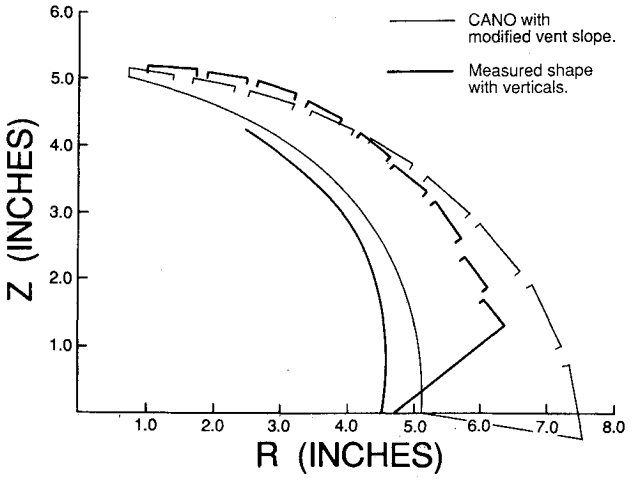

Fig. 13 Measured and calculated shapes (CANO3 modified vent slope, 5.2 lb/ft^2 dynamic pressure).

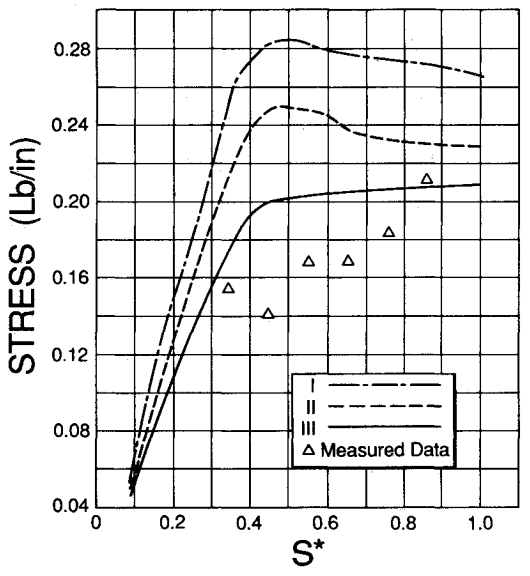

Fig. 14 Calculated and measured stress vs S^* for 7.8 lb/ft^2 dynamic pressure: I) CANO conventional vent slope, II) CANO3 conventional vent slope, III) CANO3 modified vent slope.

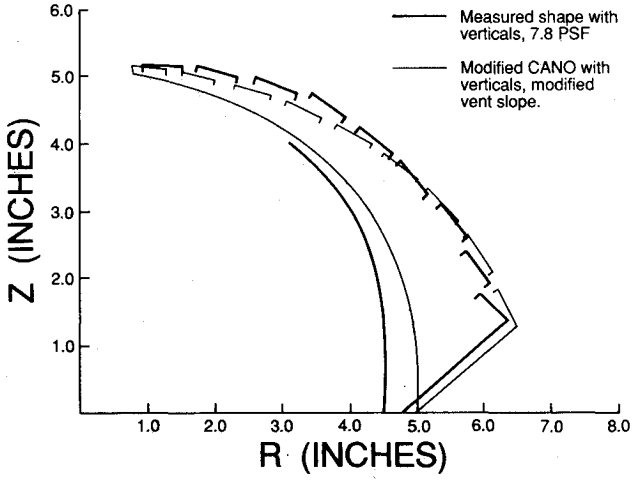

Fig. 15 Calculated and measured shapes for 7.8 lb/ft^2 dynamic pressure, CANO3, modified vent slope.

that predicted by CANO with the standard vent boundary condition, but not as close as the stress predicted by CANO with the modified vent boundary condition. Finally, the vent boundary condition on CANO3 was changed to give the best fit at the vent. The resulting shape, as shown in Fig. 13, is closest to the measured shape and the resulting stress is closest to the measured stress (see Fig. 9). It appears that, in terms of accurately predicting stress, it is most important to get the shape correct in the neighborhood of the vent. Skirt shape is less critical.

Similar results for a dynamic pressure of 7.8 lb/ft^2 are shown in Figs. 14 and 15. Figure 14 shows measured and calculated stress. The relative magnitudes of the measured and calculated stresses are about the same as for 5.2 lb/ft^2. The worst results are given by conventional CANO. CANO3 with conventional vent slope boundary conditions gives better results and CANO3 with the boundary condition modified to give the best fit to the mesured shape gives the best estimates of the stress. The excellent correspondence between the measured and calculated shapes is shown in Fig. 15. Similar results were obtained for 6.5 lb/ft^2.[23]

Conclusion

It has been shown that for the ribbon parachute tested, the stresses calculated using CANO tend to be larger than measured stresses. The shapes predicted using CANO are not very close to the measured shapes. If the vent boundary condition on CANO is changed so that the calculated and measured shapes are close, the calculated stress is much closer to the measured stress. Unfortunately, in practice, the actual shape of the parachute is usually not known; therefore, the practical applications of this technique are limited. A modified version of CANO, called CANO3, was developed that allowed simulation of verticals and resulted in a much better match of the canopy shape at the skirt. CANO3 gave better results than the original CANO without changes in the vent boundary condition, but not as good as were obtained from CANO with the vent boundary condition changed to give a good match with the measured shape near the vent. When the vent boundary condition on CANO3 was changed to give a good match of the shape near the vent, a very good correspondence between the measured and calculated stresses was obtained. In using CANO, it appears to be most important to get a good match of the shape near the vent.

The model parachute used in this study was lightly loaded. As the loading is increased, the vent area becomes flatter and the shape becomes more like that predicted by CANO using the original vent boundary condition. In this case, the calculated and measured results might be closer. It would be desirable to conduct tests at dynamic pressures higher than those obtainable in the University of Minnesota wind tunnel.

Although CANO3 appears to give better results than the original CANO, it does not converge as readily and involves a somewhat arbitrary assumption about the angles that the horizontal ribbons make with the radials. If data on the inflated shape are available, these assumptions can be adjusted to agree with the measured data. Also, the vent boundary conditions can be adjusted to give a good match with the shape at the vent and the resulting predicted stress distribution will be very close to the actual distribution.

If used within its limitations and if the results are interpreted correctly, CANO and its modifications are useful design tools and should certainly give more accurate results than simple membrane theories often used.[29] On the other hand, CANO dates from the late 1960s and early 1970s and the algorithms used appear to be designed to accommodate the memory and speed limitations of the computers of that era. Considering the enormous developments in finite-element methods and computers that have occurred since CANO was originally written, it appears time to develop a new code. This code should be able to handle parachutes

that are not necessarily axially symmetric and that are subject to biaxial stress distributions (i.e., solid parachutes).

Acknowledgment

This research was supported by Sandia National Laboratories under Contract 16-9903 and 48-1974. Dr. Carl W. Peterson was contract monitor.

References

[1]Taylor, G.I., Southwell, R., Griffiths, T., Jones, R., and Williams, J.H., "On the Aerodynamic Characteristics of Parachutes," British Aeronautical Research Committee, R&M 862, June 1923.

[2]Stevens, G.W.H. and Johns, T.F., "The Theory of Parachutes with Cords Over the Canopy," British Aeronautical Research Council, R&M 2320, July 1942.

[3]Duncan, W.J., Stevens, G.W.H., and Richards, G. J., "Theory of the Flat Elastic Parachute," British Aeronautical Research Council, R&M 2118, March 1942.

[4]Jaeger, J.A., Culver, I.H., and Della-Vedowa, R.P., "A Study of the Flat Elastic Parachute," Lockheed Aircraft Corp., Burbank, CA, Rept. 8541, Aug. 1952.

[5]Topping, A.D., Marketos, J.D., and Costakos, N.C., "A Study of the Load Distribution in a Conical Ribbon Type Parachute," AFWADC-TR-55-294, Oct. 1955.

[6]Lester, W.G.S., "A Note on the Generalization of Elastic Curves Representing Parachute Shapes," Royal Aircraft Establishment, England, Rept. N-ME-357, July 1962.

[7]Heinrich, H.G. and Jamison, L.R., "Parachute Stress Analysis During Inflation and at Steady State," *Journal of Aircraft*, Vol. 3, Jan.-Feb. 1966, pp. 52-53.

[8]O'Hara, F., "Notes on the Opening Behaviour and the Opening Forces of Parachutes," *Journal of the Royal Aeronautical Society*, Vol. 53, Nov. 1949, pp. 1053-1062.

[9]Asfour, K.J., "Analysis of Dynamic Stress in an Inflating Parachute," *Journal of Aircraft*, Vol. 4, Sept.-Oct. 1967, pp. 429-434.

[10]Ross, E.W., "Approximate Analysis of a Flat Circular Parachute in Steady Descent," *Journal of Aircraft*, Vol. 7, May-June 1970, pp. 266-271.

[11]Roberts, B.W., "A Contribution to Parachute Inflation Dynamics," AIAA Paper 68-928, Sept. 1968.

[12]Roberts, B.W., "The Shape and Stresses in an Arbitrarily Shaped Gore Parachute Under an Arbitrary Pressure Distribution," AIAA Paper 70-1197, Sept. 1970.

[13]Mullins, W.M., Reynolds, D.T., Lindh, K.G., and Bottorff, M.R., "Investigation of Prediction Methods for the Loads and Stresses of Apollo Type Spacecraft Parachutes, Vol. II: Stresses," Northrop Corp., Newbury Park, CA, Rept. NVR-6432, June 1970.

[14]Meyers, S.D., Klimas, P.C., and Wolf, D.F., "Structural Analysis and Design of a High Performance Lifting Ribbon Parachute," AIAA Paper 79-0428, March 1979.

[15]Cyrus, J.D. and Nykvist, W.K., "Retrorocket-Assisted Parachute Inflight Delivery (Rapid) Systems Study," AIAA Paper 84-0805, April 1984.

[16]Reynolds, D.T. and Mullins, W.M., "Stress Analysis of Ribbon Parachutes," AIAA Paper 75-1372, Nov. 1975.

[17]Heinrich, H.G. and Noreen, R.A., "Stress Measurements on Inflated Model Parachutes," AIAA Paper 73-445, May 1973.

[18]Heinrich, H.G. and Saari, D.G., "Parachute Canopy Stress Measurements at Steady State and during Inflation," *Journal of Aircraft*, Vol. 16, Aug. 1978, pp. 534-539.

[19]Heinrich, H.G., "Biaxial Stress Measurements on Cloth Samples and Bias Constructed Parachute Models," *Journal of Aircraft*, Vol. 17, July 1980, pp. 487-492.

[20]Wagner, P.M., "Experimental Measurement of Parachute Canopy Stress during Inflation," AFFDL-TR-78-53, May 1978.

[21]Braun, G. and Doherr, K.F., "Experiments with Omega Sensors for Measuring Stress in the Flexible Materials of Parachute Canopies," *Journal of Aircraft*, Vol. 18, Oct. 1980, pp. 358-364.

[22]Eaton, J.A., "Improvement of Temperature Characteristics of the Omega Sensor," DFVLR Rept. IB 154-79/15, Dec. 1979.

[23]Garrard, W.L., Konicke, M.L., and Wu, K.Y., "A Comparison of Measured and Calculated Stress and Shape in Parachute Canopies," Sandia National Laboratories, Albuquerque, NM, Final Report on Contract 48-1974, Aug. 1986.

[24]Henfling, J.F. and Purvis, J.W., "Pressure Distribution on Parachute Ribbon Shapes," AIAA Paper 84-0815, April 1984.

[25]Garrard, W.L., Wu, K.Y., and Muramoto, K.K., "Steady State Stresses in Ribbon Parachutes," AIAA Paper 84-0816, April 1984.

[26]Garrard, W.L. and Konicke, T.A., "Stress Measurements in Bias Constructed Parachute Canopies During Inflation and Steady State," *Journal of Aircraft*, Vol. 18, Oct. 1981, pp. 881-887.

[27]Konicke, T.A. and Garrard, W.L. "Stress Measurements in a Ribbon Parachute Canopy," *Journal of Aircraft*, Vol. 19, July 1982, pp. 598-600.

[28]Testa, R.B. and Boctor, W., "A Biaxial Stress Transducer for Fabrics," *Experimental Mechanics*, Vol. 24, March 1984, pp. 33-39.

[29]Ewing, E.G., Bixby, H.W., and Knacke, T.W., "Recovery Systems Design Guide," AFFDL-TR-78-151, Dec. 1978.